Geological Survey of Canada

CURRENT RESEARCH
2007-D1

Processing of single-channel, high-resolution seismic data collected in the St. Lawrence estuary, Quebec

M.J. Duchesne and G. Bellefleur

2007

Natural Resources Canada / Ressources naturelles Canada

Canada

CURRENT RESEARCH

ISSN 1701-4387
Catalogue No. M44-2007/D1E-PDF
ISBN 978-0-662-45061-0

A copy of this publication is also available for reference in depository libraries across Canada through access to the Depository Services Program's Web site at http://dsp-psd.pwgsc.gc.ca

A free digital download of this publication is available from GeoPub:
http://geopub.nrcan.gc.ca/index_e.php

Toll-free (Canada and U.S.A.): 1-888-252-4301

Critical reviewer
Andre Pugin

Authors

M.J. Duchesne
(mduchesn@nrcan.gc.ca)
GSC (Québec)
490 rue de la Couronne
Québec, Quebec G1K 9A9

G. Bellefleur
(gbellefl@nrcan.gc.ca)
GSC (Central Canada)
615 Booth Street
Ottawa, Ontario K1A 0E9

Publication approved by GSC Québec

Correction date:

Processing of single-channel, high-resolution seismic data collected in the St. Lawrence estuary, Quebec

M.J. Duchesne and G. Bellefleur

Duchesne, M.J. and Bellefleur, G., 2007: Processing of single-channel, high-resolution seismic data collected in the St. Lawrence estuary, Quebec; Geological Survey of Canada, Current Research 2007-D1, 11 p.

Abstract: Within the framework of the Appalachian Energy project of the Target Geosciences Initiative – Part 2, more than 3000 km of single-channel, high-resolution seismic profiles were collected with a sparker source in the St. Lawrence estuary in 2003 and 2004 to map shallow sedimentary series (sediments and the top of the underlying bedrock). The data collected include many artifacts such as short- and long-period multiples. In order to provide, as much as possible, artifact-free sections, a processing flow was developed and applied to all 55 profiles collected. The core of the ten-step flow is a trace-by-trace deconvolution algorithm which allows the compression of the source signature. The processed sections provide improved seismic images that allow accurate picking of key stratigraphic reflectors.

Résumé : Dans le cadre de la partie 2 du projet sur les ressources énergétiques des Appalaches de l'Initiative géoscientifique ciblée, nous avons utilisé un étinceleur pour obtenir plus de 3000 km de profils sismiques monotrace à haute résolution dans l'estuaire du Saint-Laurent. Ces données, recueillies en 2003 et 2004 en vue de cartographier des séries sédimentaires à de faibles profondeurs, contiennent de nombreux artéfacts, par exemple des réflexions multiples de courte et de longue périodes. Afin de fournir dans la mesure du possible des profils sans artéfacts, nous avons établi un processus à 10 étapes qui a servi pour le traitement des 55 profils obtenus. Ce processus comporte un algorithme de déconvolution trace par trace qui permet de comprimer la signature de la source. Les profils traités fournissent une image sismique améliorée qui permet de sélectionner avec précision les réflecteurs stratigraphiques clés.

INTRODUCTION

High-resolution marine seismic surveys conducted with a single-channel streamer are very attractive to marine geologists because of the easy-to-deploy character of these systems, which provide zero-offset sections almost ready for interpretation. Although these systems are relatively easy to use, they do not exclude pitfalls or artifacts on the sections. Hence, advanced processing is still needed, but also is often ignored because of the cost and the time associated with it. Therefore, seismic interpretation is often done with the annoying presence of artifacts, which sometimes leads to misinterpretations (Tucker, 1982; Sylwester, 1983). This technical note reviews the steps of a processing flow developed for single-channel high-resolution marine seismic data gathered with a low-energy sparker source in the St. Lawrence estuary. One objective of the processing flow is to homogenize the stratigraphic response on all profiles to help interpretation.

SPARKER SOURCE

The sparker is a marine impulsive source frequently used for high-resolution seismic surveys requiring 0.5 to 10 m of vertical resolution (Mosher and Simpkin, 1999). Sparker sources were very popular during the late 1960s and the 1970s before being supplanted by small-volume airguns (Trabant, 1984). Since the last decade, there has been a regain of interest in sparker technology because 1) it can be easily deployed at relatively low cost, and 2) in certain areas the use of small airguns is restricted due to environmental concerns (e.g. Aarseth et al., 1997; Ceramicola et al., 2002; Pichevin et al., 2003; Labaune et al., 2005, and Llave et al., 2006).

Sparker sources work by discharging a high-voltage electrical current between electrodes in a conducting fluid (i.e. salt water). This vaporizes the water, leading to the growth and the collapse of cavities (bubbles) due to the static pressure becoming smaller than the fluid vapour pressure (Sheriff, 2005). The implosion of the cavities creates the shock wave. The expansion of water and gases produced by an underwater spark creates a low-pressure region that eventually collapses to generate the bubble effect.

Sparker systems have the reputation of generating long and complex seismic signatures (Fig. 1; Verbeek and McGee, 1995; Mosher and Simpkin, 1999). The secondary bubbles created by the sparker signals interfere destructively and strongly attenuate amplitudes at some frequencies of interest (Fig. 2; Mosher and Simpkin, 1999). In addition, variable discharge paths associated with the array of electrodes tends to add more complexity to the sparker signature. It is common to observe a pulse train of 25 to 50 ms with a secondary pulse which has larger amplitudes than the primary pulse (Fig. 1; Trabant, 1984; Cannelli and D'Ottavi, 1991). The presence of a long pulse train masks reflections immediately below the seafloor and underneath subsequent reflectors (Trabant, 1984).

SEISMIC DATA

Seismic data were collected to assess the stratigraphy of Quaternary sediments, to locate areas with free gas, and to provide information on shallow structures and lithologies of

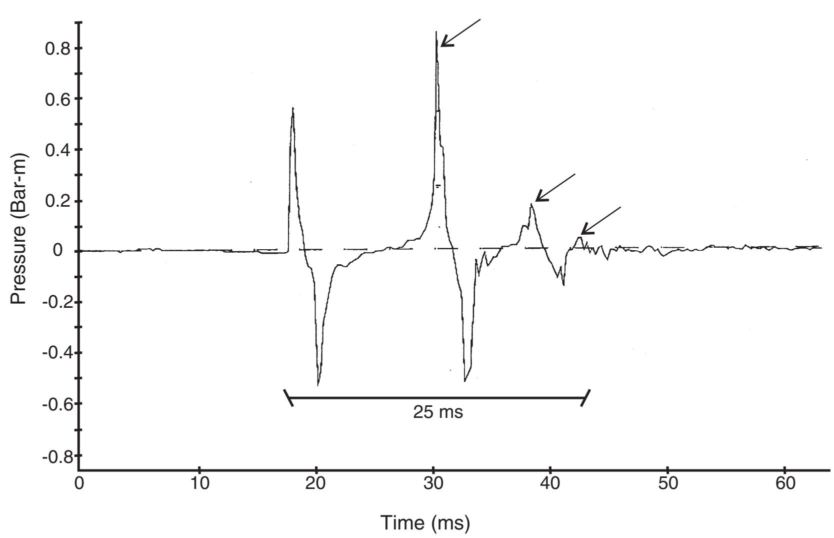

Figure 1. Acoustic signature of an 8 kJ sparker-array (courtesy of D.C. Mosher). Arrows denote the position of the secondaries.

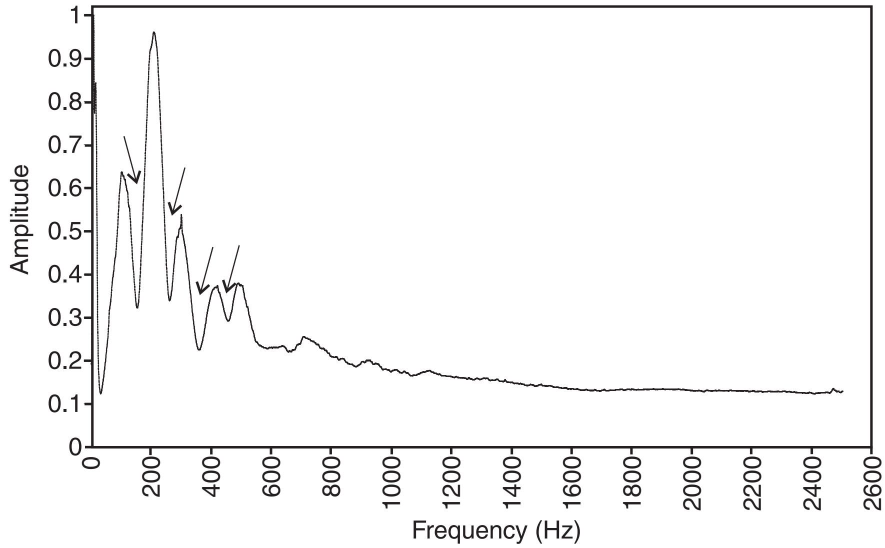

Figure 2. Amplitude spectrum of the raw data used in this study. Arrows are pointing at some frequencies notched due to the presence of secondary bubbles.

the bedrock in the St. Lawrence estuary (Bellefleur et al., 2006). A total of 3300 km of single-channel, high-resolution seismic data were collected along 55 profiles during two cruises in 2003 and 2004 onboard the *RV Coriolis II* (Table 1, Fig. 3). Seismic traces were shot with a 4.5 kJ EG & G sparker array (nine electrodes) with a frequency centred on 200 Hz (Fig. 2). The source was fired as a function of time (i.e. every 4 s) producing an average trace spacing of 10 m. The traces were recorded with a 12 m long single channel streamer combining the signal of 23 elements. The source was towed 25 m behind the ship's stern at a depth of about 5 m whereas the streamer was surface-towed (no 'bird' was available) 25 m behind the source (Fig. 4). Data having a vertical resolution of approximately 5 ms were recorded on a 1.25 s trace length and originally sampled at 20 µs before being resampled to 200 µs for computing purposes. The source signal includes four different seismic events spread over about 30 ms, of which three are secondary arrivals. The presence of the secondary arrivals indicates that every single reflection is triplicated. Unfortunately no single hydrophone was available to record the acoustic signature of each shot.

Table 1. Acquisition parameters for the seismic data

Source	EG&G 9-electrodes sparker array
Fire rate	4 s
Energy	4.5 kJ
Peak frequency	200 Hz
Streamer	IKB single-channel
Length	12 m
Number of hydrophones	23
Data format	Digital SEG-Y
Vertical resolution at the seafloor	~5 ms
Trace length	1.25 s
Sample rate	1 sample every 20 μs

PROCESSING FLOW

The major processing challenges were the attenuation of the strong secondaries produced by the sparker source and the attenuation of the long-period multiples associated with the seafloor and bedrock seismic events. The presented flow suits most the processing needs identified for the raw data, and was developed with the processing tools available in-house. One representative section (04C-9) has been selected to illustrate the effect of the main processing steps on the data (Fig. 5). Each step of the processing flow is reviewed in this section and summarized in Table 2. All sections were processed with VISTA 2-D seismic processing package (version 5.5) on a PC machine equipped with a single 3.20 GHz Xeon CPU and 3.5 GB of RAM.

First, all traces were muted between 0 ms to the seafloor reflections (Table 2). The mute function eliminates the relative contribution of the direct arrivals and the noise present in the water column that may affect further processing steps.

Secondly the seafloor reflection was picked on each trace and saved in the headers of the SEG-Y file. Picks are used in some of the following processing steps and are particularly useful to flatten the data.

The third step corresponds to the application of a spherical-divergence correction which compensates for the decrease in wave strength (energy per unit area of wavefront) with distance as a result of geometric spreading (Sheriff, 2005). Geometrical spreading law states that the energy density decreases inversely as the square of the distance the wave has travelled, which means that the amplitude decreases linearly with the distance travelled. The distances are estimated from two velocity analyses obtained from multichannel profiles 04C-5 and 04C-15, also collected in the estuary (Fig. 4). Both analyses show weak velocity contrasts between the unconsolidated sedimentary units, with velocities ranging from 1485 to 1600 m/s. A constant velocity of 1520 m/s is representative

Table 2. Processing flow and parameters for section 04C-9

Processing step	Parameters used
Mute	0 ms to first arrival
First arrival picking	Pick trough, search window: 2 ms, pick to nearest ½ sample rate, picked events recorded in SEG-Y header rc_stat (integer, first byte: 101)
Spherical divergence correction	Time 1: 0 ms velocity 1520 m/s, time 2: 1250 ms velocity 1520 m/s
Time-variant spectrum balancing	Bandwith: 30 Hz, slope: 50 Hz, top frequence: 380 Hz
Ormsby band-pass filter	f_1: 30 Hz f_2:60 Hz f_3: 330 Hz f_4: 380 Hz
Flatten	First arrival flattened to 0 ms from SEG-Y header rc_stat
Trace-by-trace decon design (based on VSP downgoing decon)	Operator length: 40 ms (time: 0 ms), positive side: 40 ms, negative side: 40 ms, operator taper: 20 ms, pre-whitening noise: 1%
Time-variant predictive deconvolution	Operator length: 1000 ms (time: 0 ms), operator taper: 20 ms, pre-whitening noise: 1%, prediction lag: first arrival from SEG-Y header rc_stat
Static shift	All traces shifted on first arrival from SEG-Y header rc_stat (integer, first byte: 101)
AGC	Window: 100 ms, scale: 1, Initial hard zero: skipped

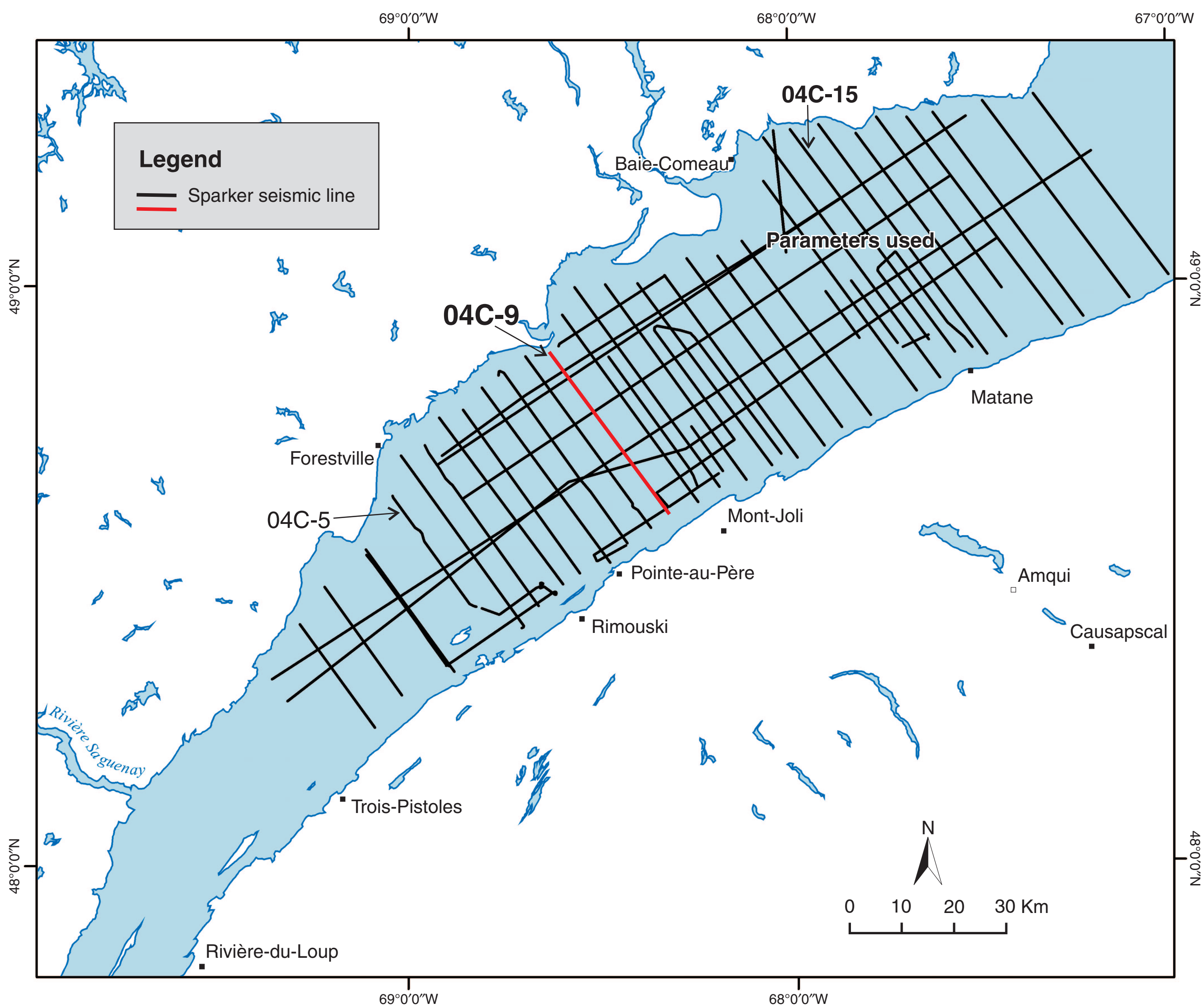

Figure 3. Location of the seismic sections. Section 04C-9, shown in red, is used as an example in Figures 5 to 8.

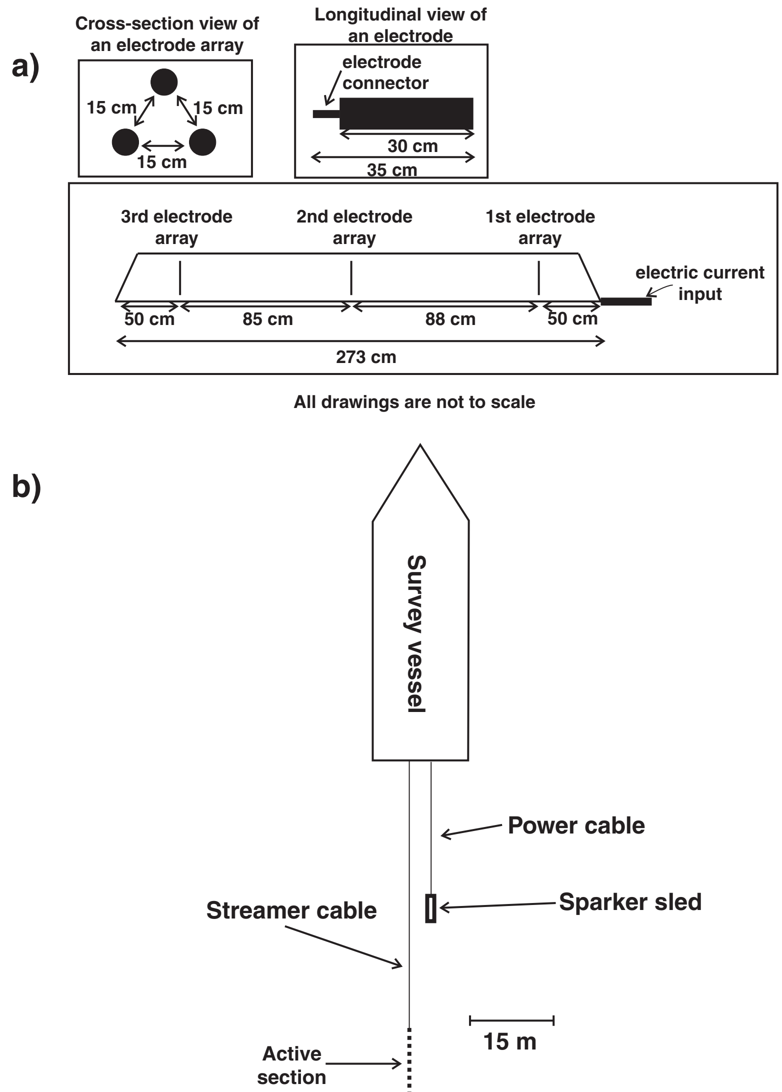

Figure 4. Geometry of **a)** the sparker-array, and **b)** the acquisition system.

of the shallow stratigraphy (sediments and the top of the underlying bedrock) and was used for the spherical divergence correction (*see* Bellefleur et al., 2006).

The fourth step is the time-variant spectrum-balancing algorithm which is used to equalize the spectrum of all traces (Claerbout, 1975; Coppens and Mari, 1984). For this study, the spectrum balancing was employed to pull out notches present in the amplitude spectrum due to the occurrence of secondary bubbles (Table 2, Fig. 2).

This was followed by the application of an Ormsby band-pass filter (step 5, Table 2). This filter has a typical trapezoidal shape defined by four corner frequencies: a low truncation (f_1), a low cut (f_2), a high cut (f_3), and high truncation (f_4). Corner frequencies (30-60-330-380 Hz) were determined based on the amplitude spectrum of all surveys.

The sixth step consisted in the flattening of the seafloor reflection to 0 ms using the picks from the second processing step. The flattening facilitates the choice of design windows and was utilized in the two following steps; namely for a trace-by-trace source deconvolution and a predictive deconvolution.

The trace-by-trace source deconvolution (step 7) was applied to attenuate lateral and time variations introduced by the complex signature of the sparker. In the Vista software, trace-by-trace deconvolution is applied using the VSP (vertical seismic profile) deconvolution tool. Thus, each trace of the profile was processed as if it was part of a VSP record. It is the flexibility of this approach that has allowed its use on standard seismic profiles rather than its intrinsicture.

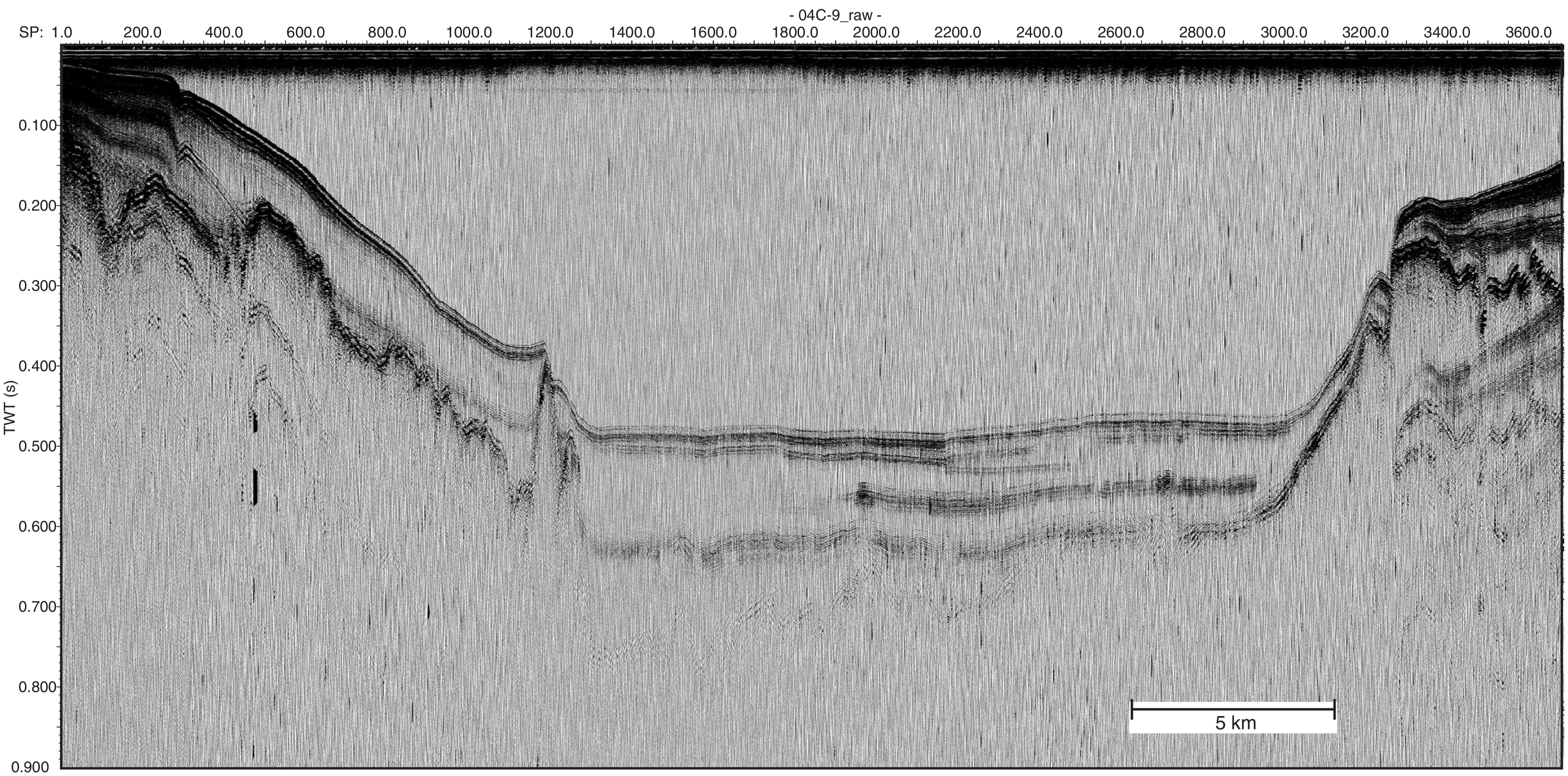

Figure 5. Raw section 04C-9. *See* Figure 3 for location of Section 04C-9.

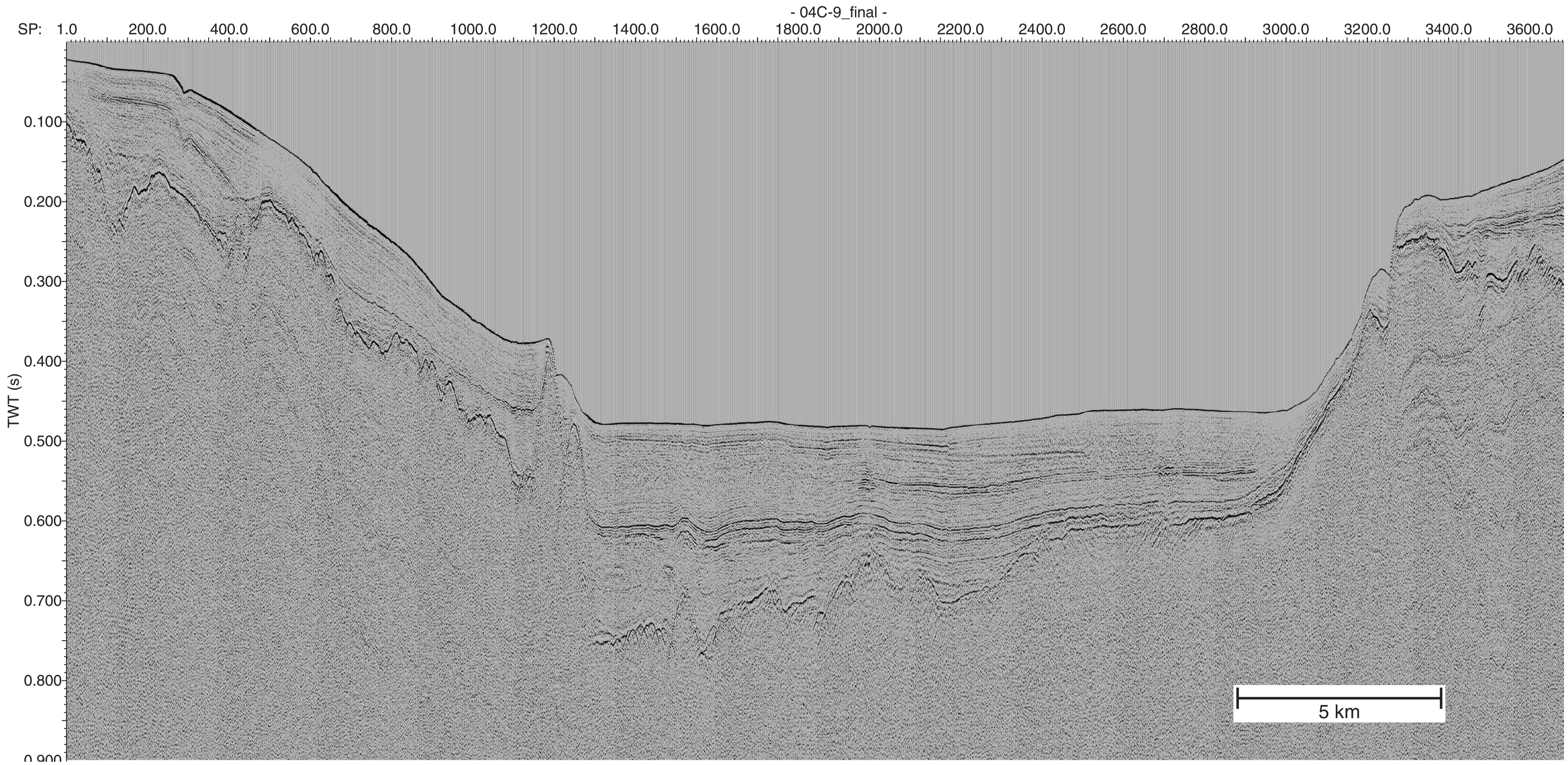

Figure 6. Section 04C-9 after the application of the entire processing flow. *See* Figure 3 for location of Section 04C-9.

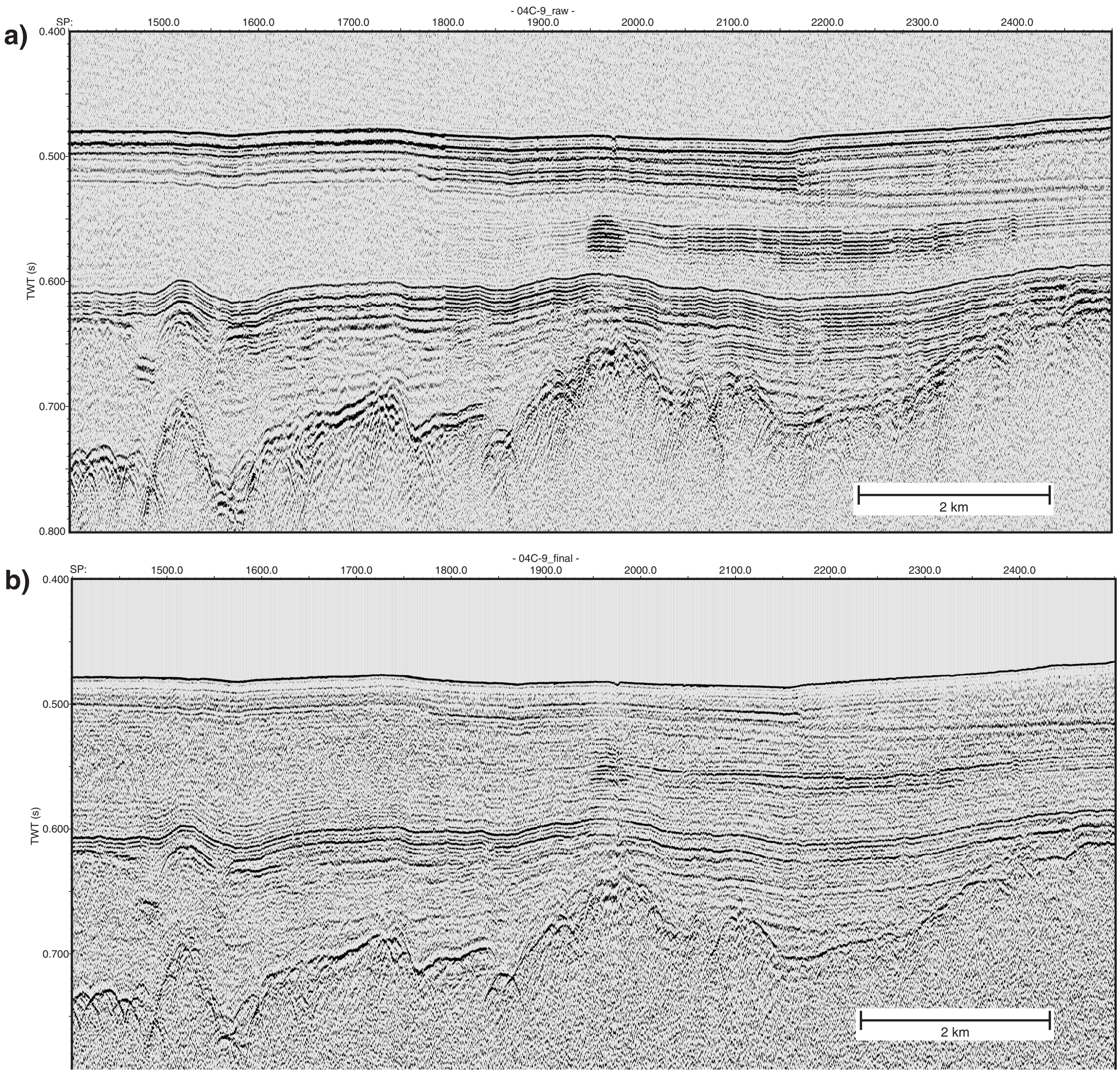

Figure 7a) Raw portion of profile 04C-9 and **b)** processed version of the same portion. The VSP deconvolution permitted the efficient compression of the sparker secondaries. *See* Figure 3 for location of Section 04C-9.

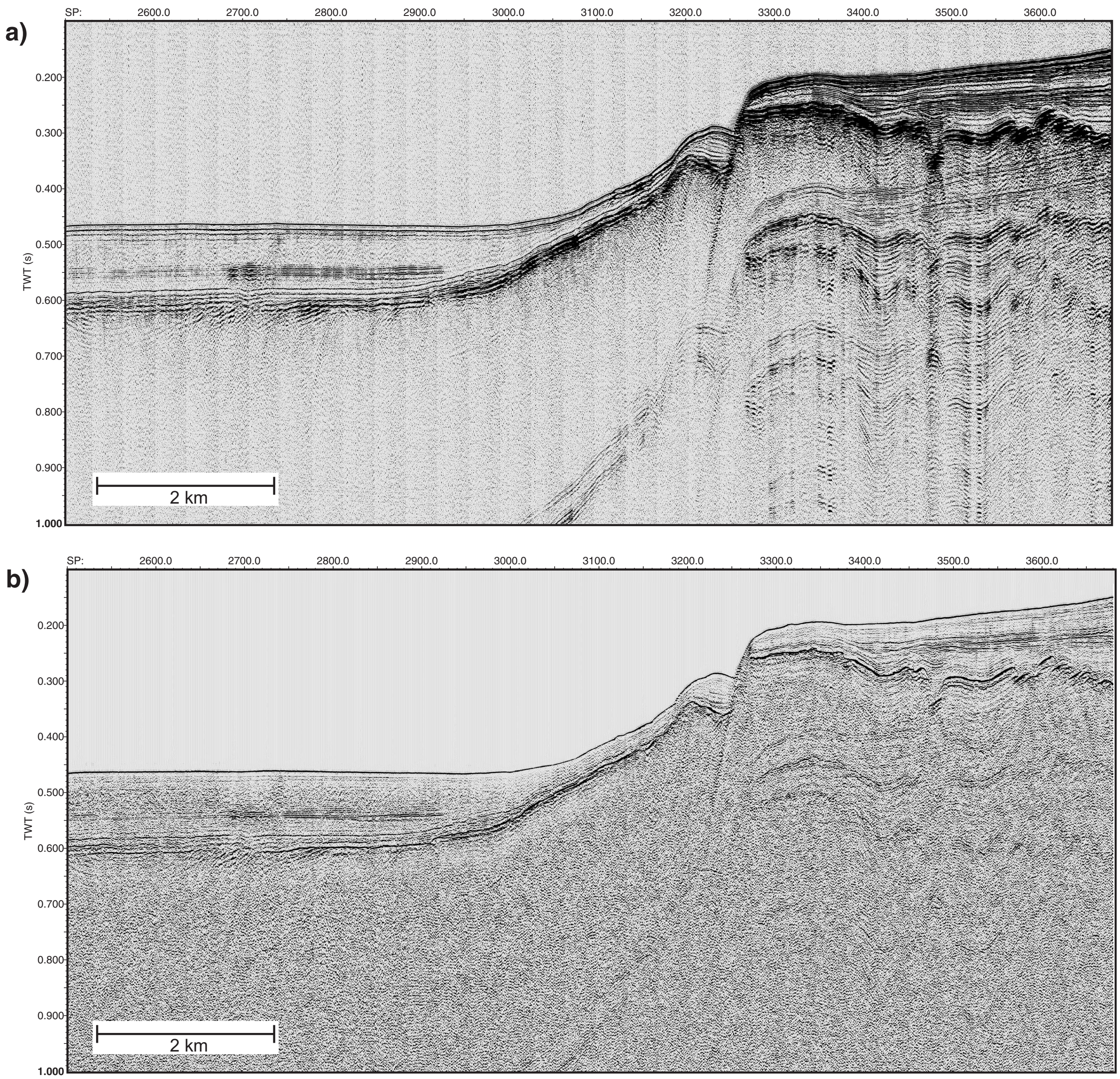

Figure 8a) Raw portion of profile 04C-9 and **b)** processed version of the same portion. The time-variant deconvolution significantly attenuated the energy of the long-period multiples associated with seafloor and bedrock reflections. *See* Figure 3 for location of Section 04C-9.

The main task pursued by the time-variant predictive deconvolution (step 8) is the removal or the attenuation of long-period multiples associated with seafloor and bedrock events (Table 2). The operator involves a prediction process based on the knowledge of the two-way traveltime of the primaries related to the same reflectors (Sheriff and Geldars, 1995; Yilmaz, 2001). In trace-variant predictive deconvolution a different lag is set for each trace. The general assumption that the first seafloor multiple appears at twice the time-depth of the seafloor primary is used to set the lag of the prediction. The length of the operator was set to 1000 ms to catch all long-period multiples present on the seismic profile. After predictive deconvolution, the data was put back to their original time (step 9) using the reverse of the operation described in processing step 6.

Finally, the last step is the application of an automatic gain control (AGC) function on the data (Table 2). It was mostly used to improve visibility of late-arriving events in which attenuation has caused amplitude decay.

RESULTS

In general, results obtained with the application of the processing routine provided satisfactory results (Fig. 6). Only a few sections with initial low signal-to-noise ratios did not show significant improvement after processing. The trace-by-trace source deconvolution provided the flexibility needed to handle the shot-to-shot variation of the sparker signature and led to the efficient compression of the long pulse train of the wavelet (Fig. 7).

In the St. Lawrence estuary, the strong imprint of long-period multiples on seismic sections is not new and has been observed on previous seismic surveys (SOQUIP, 1987). The time-variant predictive deconvolution function allowed dealing with rapidly changing water depths along the section, a characteristic that would limit the performance of a constant lag prediction. Most of the energy contained within multiple reflections has been greatly attenuated by the time-variant predictive deconvolution (Fig. 8). However, the algorithm failed to significantly reduce the presence of high-energy multiples contained on the shallow portions of some sections.

The time-variant spectrum balancing helped to equalize the amplitude spectrum of the raw data. As a result, the bandwidth and signal-to-noise ratio have been enhanced and the resolution of the seismic image improved.

CONCLUDING REMARKS

The application of the processing flow provided clearer seismic images for interpretation. The ambiguity initially observed for some horizons has been removed after compression of the sparker source wavelet. This facilitates the stratigraphic correlation between different profiles. The attenuation of long-period multiples should help to depict reflection adjoined to primaries from artifacts, particularly in the shallower parts of the profiles. Nevertheless, because of the deconvolution processes, some stratigraphic seismic events interfering with secondaries were either attenuated or suppressed. The energy of the primary could not be separated from the multiples because both seismic events were overlapping. Therefore, the application of the deconvolution operators locally introduced amplitude blanking on the data at the time-depths where the multiples were observed. In the present case, secondaries were included in an approximately 30 ms long time window and inverse filtering operators were all 40 ms long. Unfortunately the loss of seismic stratigraphic information due to the compression of the source signal was necessary to allow more accurate imaging of key seismic events.

Most of the processing effort was directed towards the attenuation of the strong secondaries produced by the sparker. A modern source such as a double-chamber GI airgun should be considered in future surveys to minimize any source-related problems. With the availability of a source that could provide a shorter pulse, the data processing could have been carried in a timely and cost-effective manner.

ACKNOWLEDGMENTS

The authors thank Érick Adam (Hydro-Québec Pétrole et Gaz) for his technical advice during the early stages of the development of the processing flow. The guidance of Mike Galbraith, Randy Kolesar, and Rick Kuzmiski (Geophysical Exploration and Development Corporation) regarding the functioning of VISTA throughout the elaboration of the processing routine was greatly appreciated. Nicolas Pinet (GSC-Québec) is thanked for his comments concerning the various algorithms tested during the course of the flow development. The authors are thankful to all scientific and support staff who participated to the single-channel data acquisition on the two seismic cruises. M.J. Duchesne and G. Bellefleur are also in debt to the officers and the crew of *RV Coriolis II.* The financial contribution of Hydro-Québec Pétrole et Gaz is also acknowledged.

REFERENCES

Aarseth, I.
1997: Western Norwegian fjord sediments: age, volume, stratigraphy, and role as temporary depository during glacial cycles; Marine Geology, v. 143, p. 39–53

Bellefleur, G., Duchesne, M.J., Hunter, J., Long, B.F., and Lavoie, D.
2006: Comparison and processing of single and multi-channel high-resolution seismic data for shallow stratigraphy mapping in the St. Lawrence Estuary; Current Research 2006-D2, 10 p.

Cannelli, G.B. and D'Ottavi, E.
1991: High-power acoustic-wave system for marine environment surveying; Oceans, v. 1, p. 482–487.

Ceramicola, S., Rebesco, M., De Batist, M., and Khlystov, O.
2002: Seismic evidence of small-scale lacustrine drifts in Lake Baikal (Russia); Marine Geophysical Researches, v. 22, p. 445–464.

Claerbout, J.F.
1975: Spectral balancing; Stanford Exploration Project Report no. 7, p. 172–182

Coppens, F. and Mari, J.L.
1984: L'égalisation spectrale: un moyen d'améliore la qualité des données sismiques; Geophysical Prospecting, v. 32, p. 258–281.

Labaune, C., Jouet, G., Berné, S., Gensous, B., Tesson, M., and Delpeint, A.
2005: Seismic stratigraphy of the deglacial deposits of the Rhône prodelta and adjacent shelf; Marine Geology, v. 222-223, p. 299–311.

Llave, E., Schönfeld, J., Hernandez-Molina, F.J., Mulder, T., Somoza, L., Diàz Del Rio, V., and Sanchez-Almazo, I.
2006: High-resolution stratigraphy of the Mediterranean outflow contourite system in the Gulf of Cadiz during the late Pleistocene: the impact of Heinrich events; Marine Geology, v. 227, p. 241–262.

Mosher, D.C. and Simpkin, P.G.
1999: Status and trends of marine high-resolution seismic reflection profiling: data acquisition; Geoscience Canada, v. 26, p. 174–188.

Pichevin, L., Mulder, T., Savoye, B., Gervais, A., Cremer, M., and Piper, D.J.W.
2003: The Golo submarine turbidite systems (east Corsica margin): morphology and processes of terrace formation from high-resolution seismic profiles; Geo-Marine Letters, v. 23, p. 117–124.

Sheriff, R.E.
2005: Encyclopedic dictionary of applied geophysics; Society of Exploration Geophysicists, Tulsa, Oklahoma, 429 p.

Sheriff, R.E. and Geldart, L.P.
1995: Exploration Seismology; Cambridge University Press, Cambridge, United Kingdom, 592 p.

SOQUIP (Société Québécoise d'Initiatives Pétrolières)
1987: Estuary and Gulf of St. Lawrence, geological-geophysical-geochemical data integration; Geological Survey of Canada, Open File Report 1721, 75 p.

Sylwester, R.E.
1983: Single-channel, high-resolution, seismic-reflection profiling: a review of the fundamentals and instrumentation; *in* Handbook of Geophysical Exploration at Sea, (ed.) R.A. Greyer; CRC Press, Boca Raton, Louisiana, p. 77–122.

Trabant, P.K.
1984: Applied high-resolution geophysical methods: offshore geoengineering hazards; International Human Resources Development Corporation, Boston, Massachusetts, 265 p.

Tucker, P.M.
1982: Pitfalls revisited; Society of Exploration Geophysicists, Tulsa, Oklahoma, 23 p.

Verbeek, N.H. and McGee, T.M.
1995: Characteristics of high-resolution marine reflection profiling sources; Journal of Applied Geophysics, v. 33, p. 251–269.

Yilmaz, O.
2001: Seismic data analysis: processing, inversion and interpretation of seismic data; Society of Exploration Geophysicists, Investigations in Geophysics No.10, Tulsa, Oklahoma, 2027 p.

Geological Survey of Canada Project Y53